Progress in Organic Coatings 108 (2017) 25–29

Contents lists available at ScienceDirect

Progress in Organic Coatings

journal homepage: www.elsevier.com/locate/porgcoat

Enhancement of barrier properties by wet coating of epoxy-ZrP nanocomposites on various inorganic layers

Haesook Kim[a], Ha Na Ra[a], Mansu Kim[a], Hyun Gi Kim[a,b], Sung Soo Kim[a,b,*]

[a] Regional Innovation Center for Components and Materials for Information Display, Kyung Hee University, Yongin-si, Gyeonggi-do 17104, South Korea
[b] Department of Chemical Engineering, Kyung Hee University, Yongin-si, Gyeonggi-do 17104, South Korea

ARTICLE INFO

Keywords:
Epoxy nanocomposites
α-zirconium phosphate
Barrier properties
Wet coating

ABSTRACT

Epoxy-ZrP (α-zirconium phosphate) nanocomposites were wet-coated on various inorganic layers to improve their barrier properties. Inorganic layers were deposited on a plastic substrate by sputtering or atomic layer deposition (ALD). The water vapor transmission rate (WVTR) of the inorganic layers varied from 10^{-1} g/m^2/day to 10^{-4} g/m^2/day. ZrP nanoplatelets were synthesized using a reflux method and were well dispersed to form an epoxy-ZrP solution for wet coating. TEM images confirmed that the ZrP nanoplatelets were well dispersed in the epoxy matrix. The coating solution was bar-coated on the inorganic layer and thermally cured. The WVTR dramatically decreased up to 92% after epoxy-ZrP nanocomposite coating on all choices of inorganic layer. The optical properties remained constant or in some cases decreased by about 4%. The optimal structure composed of inorganic and epoxy-ZrP nanocomposite layers was used in OLED encapsulation, resulting in an extended lifetime compared to OLEDs encapsulated with bare inorganic layers without a nanocomposite coating.

1. Introduction

Flexible electronics are a fast-growing industry that has the opportunity to provide novel and advanced technologies in the future. If glass substrates are replaced by plastic films, electronic devices such as displays, solar cells, batteries, and sensors can be made flexible, lightweight, and freeform. However, since most plastic films have poor barrier properties, flexible electronics fabricated on those plastic substrates can deteriorate significantly due to the permeation of water vapor and oxygen. In particular, flexible organic light emitting diodes (OLEDs) require an ultra-low level of permeation. Therefore, many groups have researched highly advanced barrier layers that can meet such requirements. Inorganic layers deposited by sputtering, chemical vapor deposition (CVD), and atomic layer deposition (ALD) are considered the most promising options for the permeation barrier layers [1–3]. We previously researched the barrier properties of a nanolaminate of Al_2O_3/ZrO_2 as well as a single Al_2O_3 layer deposited by plasma enhanced ALD (PE-ALD) [4]. However, since the inorganic barrier layer was brittle and various unexpected defects were introduced during the deposition process, their barrier properties could decrease when they are applied to flexible substrates. To overcome these drawbacks, a flexible organic layer can be mixed into the more brittle inorganic layer to form an organic-inorganic hybrid structure.

Danforth et al. reported a UV-curable top coat protective layer to preserve the ALD film's barrier properties against downstream mechanical abrasion. They concluded that an acrylic top coat was sufficient to maintain a barrier performance with a less than 3×10^{-3} g/m^2/day water vapor transmission rate (WVTR) [5]. Kim et al. reported that hybrid encapsulation consisted of a silicon oxide/alumina and parylene layer yields an effective WVTR as low as $2.4 \pm 1.5 \times 10^{-5}$g/m^2/day. They claimed that an epoxy top coat of suitable thickness was a promising way to overcome the mechanical limitation of the inorganic barrier layer [6]. Spee at al. reported that a hybrid structure with a hot wire CVD (HWCVD) inorganic layer and initiated CVD (iCVD) organic layer showed a WVTR as low as 5×10^{-6} g/m^2/day at 60 °C and 90% relative humidity (RH). They concluded that barrier function can either be increased by combining this type of layer with slightly more flexible barrier materials such as SiO_xN_y or by stacking multiple layers using defect-decoupling strategies [7].

Of these organic layer materials, polymer nanocomposites consisting of a polymer matrix and reinforcing nanofillers are the most promising. In general, the shape, morphology, and dispersion of those nanofillers in the polymer matrix are the key factors affecting their mechanical and barrier properties [8]. In particular, it is well known that layered nanofillers such as clay [9] or graphene [10] can lengthen the pathway for the gas permeants due to increased tortuosity.

In this study, several types of inorganic layers deposited on plastic substrates such as PET or PEN were protected by a polymer nanocom-

* Corresponding author at: Department of Chemical Engineering, Kyung Hee University, Seochun-dong, Kiheung-gu, Yongin-si, Gyeonggi-do, 17104, South Korea.
E-mail address: sungkim@khu.ac.kr (S.S. Kim).

http://dx.doi.org/10.1016/j.porgcoat.2017.04.001
Received 19 January 2017; Received in revised form 23 March 2017; Accepted 2 April 2017

posite coating. Those inorganic barrier layers were prepared by sputtering or ALD methods and had WVTR values between 10^{-1} g/m^2/day and 10^{-4} g/m^2/day. The effect of polymer nanocomposites on the barrier properties of several types of inorganic layers was investigated in terms of the decoupling of existing defects in the inorganic layers. The polymer nanocomposites were successfully used as a top-coating layer to enhance the barrier properties of each inorganic layer. In addition, the lifetimes of OLED devices prepared using inorganic layers with or without polymer nanocomposite coatings were characterized.

2. Experimental

2.1. Materials

Zirconyl chloride ($ZrOCl_2 \cdot 8H_2O$, 98%, Sigma-Aldrich) and phosphoric acid (85%, Sigma-Aldrich) were used to synthesize α-zirconium phosphate (α-ZrP). The epoxy matrix was composed of bisphenol A–type epoxy resin (YD-115J) and phenoxy resin (YP-50EK35), which were purchased from Kukdo Chemical. Methyl ethyl ketone (MEK, Daejung Chemical and Metals) was used as a solvent for the coating solution. Jeffamine D-230 from Huntsman Chemical was used as a curing agent. Sputter-coated barrier films with WVTR values varying from 10^{-1} g/m^2/day to 10^{-3} g/m^2/day were received, and ALD samples with a WVTR of 10^{-4} g/m^2/day were prepared in our lab.

2.2. Preparation of α-zirconium phosphate

α-ZrP was synthesized by a reflux method [11]. Zirconyl chloride was dissolved in deionized water and added dropwise to 12 M phosphoric acid while stirring. The mixture was refluxed at 130 °C for 24 h. The resulting white suspension was rinsed with deionized water and centrifuged three times, then dried in a convection oven at 80 °C for 24 h. Thus obtained products were ground into fine ZrP particles with an average lateral diameter of 450 nm.

2.3. Preparation of epoxy-ZrP nanocomposite coating layer

α-ZrP powder was mixed in MEK for 1 h and passed through a high-pressure homogenizer (Nano Disperser, Ilshin Autoclave) to achieve better dispersion. The α-ZrP dispersion was added dropwise into the epoxy resin (YD-115J) and mechanically stirred for 6 h at room temperature. Then, the epoxy-ZrP nanocomposite mixture was blended with phenoxy resin (YP-50EK35) in the same ratio as the epoxy resin at 60 °C for 4 h. Curing agent Jeffamine D-230 was added at a stoichiometric ratio to the epoxy-ZrP nanocomposite solution and homogenized by stirring at 60 °C for 30 min. The solution was coated on the inorganic barrier layer using a bar coater and cured in an oven at 80 °C for 2 h. The content of α-ZrP in the epoxy matrix was optimized to 5 wt% as established by previous experiments, and a pure epoxy coating was tested for comparison. The thickness of the epoxy-ZrP nanocomposite coating layer was about 1–2 μm.

2.4. Fabrication of OLEDs

In order to investigate the effect of the prepared barrier structures on the lifetime of OLEDs, we fabricated OLEDs with various encapsulations. Patterned indium tin oxide (ITO, workfunction: ~4.8 eV, thickness: ~190 nm) on a glass substrate (3 cm × 3 cm) was used for the anodes of the OLEDs. ITO-coated substrates were cleaned with acetone and isopropyl alcohol in an ultrasonic bath and dried in a convection oven. Cleaned ITO was pre-treated with oxygen plasma and loaded in a high-vacuum chamber (below 3×10^{-6} Torr). Organic and metal layers were deposited by vacuum thermal evaporation. The OLEDs had an active area of 9 mm^2 and a configuration of ITO/HTL (NPB, 20 nm)/EML (Bebq2:C545T, 30 nm)/ETL (Bebq2, 20 nm)/LiF (1 nm)/Al (100 nm). The encapsulation of OLEDs was carried out using an inorganic barrier film with or without the epoxy-ZrP nanocomposite coating and a glass lid. The lifetimes of OLEDs were measured using an IVL electroluminescence characterization system (IVL 300, JBS International) under ambient conditions.

2.5. Characterization

There are several methods to measure the WVTR values of the barrier films. Mocon Inc. developed the commercial test equipment, PERMATRAN, to measure the WVTR value by using an infrared sensor, and it is commonly used in this field. However, it has a detection limit below 5×10^{-3} g/m^2/day. For the sample below the detection limit, Ca cell test has been developed. Ca cell test is based on the measurement of the electric resistance change of Ca cell depending on the degree of Ca degradation by water permeation. Ca cell test has been widely used due to its advantages; relatively low cost, easily adaptable to various environmental conditions, and real time measurable at transient and steady states under environmental stress [12].

In this work, WVTR values of the barrier films were measured by using PERMATRAN-W 3/33 or by Ca cell test depending on the level of WVTR values. Ca cell test was performed for barrier coatings with ultralow permeability below the detection limit of PERMATRAN. Results from both measrement methods were in good agreement for us to rely on the data for comparison. For preparation of Ca cell a 200nm-thick Ag electrode and a 350nm-thick Ca layer (30 × 30 mm^2 area) were sequentially deposited on a glass substrate by the thermal evaporation process. The Ca layer was encapsulated with barrier coating films using edge sealing materials. The tests were performed using two electrodes connected by a SMU probe to a Keithley 2400 source meter to measure the resistance at 38 °C and 90% RH [13]. The illustration of experimental setup for Ca test was inserted in Fig. 2(a).

The cross-sectional morphology of the epoxy-ZrP nanocomposite coating layer was observed by transmission electron microscopy (TEM, Tecnai G2 F30 S-Twin, FEI) operating at an accelerating voltage of 300 kV. A focused ion beam (FIB) system (NOVA 200, FEI) was used to prepare the samples for TEM imaging. The optical properties of transmittance and haze were measured using a UV/Visible spectrometer (MCPD-3000, Otsuka) with a wavelength range of 380 nm to 780 nm and a haze meter (NDH 5000, Nippon Denshoku), respectively.

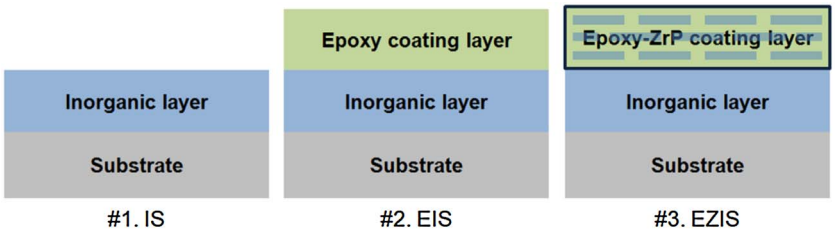

Fig. 1. A schematic diagram of each layered structure; IS (inorganic layer/substrate), EIS (epoxy coating/inorganic layer/substrate), and EZIS (epoxy-ZrP nanocomposite coating/inorganic layer/substrate).

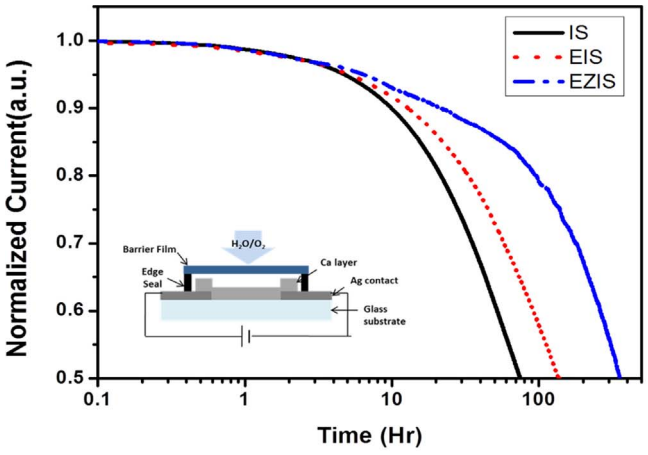

(a)

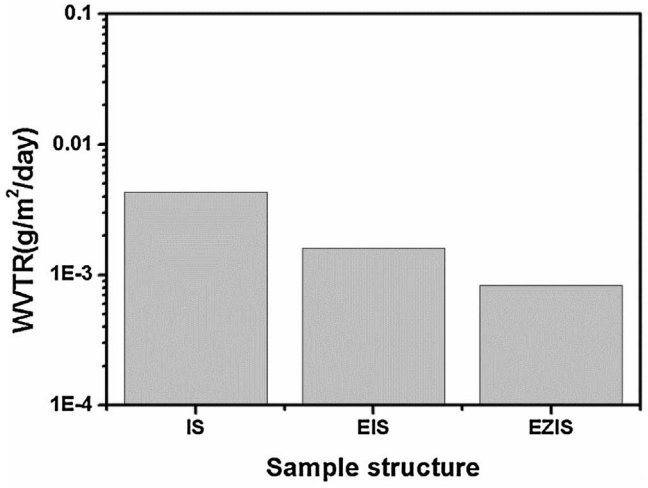

(b)

Fig. 2. (a) Normalized current-time characteristics of Ca test (38 °C, 90% RH) (b) WVTR values of IS, EIS, and EZIS samples. The inset shows an illustration of experimental setup of Ca test.

3. Results and discussion

To investigate the effect of epoxy-ZrP nanocomposite coating on the barrier properties of inorganic layers deposited on PET by the sputtering method, we tested three different structures, as shown in Fig. 1. They were categorized into samples named IS (inorganic layer/substrate), EIS (epoxy coating/inorganic layer/substrate), and EZIS (epoxy-ZrP nanocomposite coating/inorganic layer/substrate). Fig. 2(a) shows the Ca test results for all three samples by plotting normalized current versus time curves and Fig. 2(b) shows the WVTR values calculated from the slope of each curve. As shown in Fig. 2(a), Ca degradation was delayed after epoxy and epoxy-ZrP nanocomposite coating on sputtered inorganic layer. The WVTR of the IS sample dramatically decreased from 4.3×10^{-3} g/m^2/day to 1.3×10^{-3} and 8.3×10^{-4} g/m^2/day for EIS and EZIS samples, respectively. These results indicate that the top coating layer could effectively protect the inorganic layer from defects such as crack and pinhole, which cause a reduction in barrier performance [14–16].

The WVTR of the EZIS sample showed the best results to reveal that addition of α-ZrP nanoplatelets to epoxy resin still enhanced the barrier properties of the sample. α-ZrP nanoplatelets usually have layered tactoid structure, and they should be exfoliated or intercalated for good dispersion in the epoxy matrix. They must be aligned in the film plane

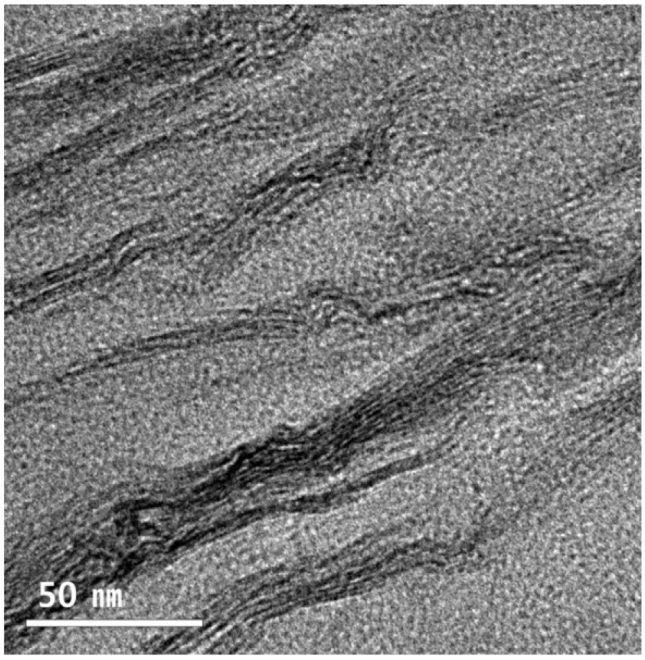

Fig. 3. Cross-sectional TEM image of the epoxy-ZrP nanocomposite coating layer.

which is perpendicular to permeation direction, to extend the pathway of permeants through a barrier layer [17]. It was confirmed from cross-sectional TEM image of the EZIS sample (Fig. 3) that α-ZrP nanoplatelets were well aligned in the film plane with no aggregation. Average length of nanoplatelets were around 450 nm and aspect ratio ranged from 100 to 500 depending on the number of layers. Even though α-ZrP nanoplatelets were not fully exfoliated and have a few layered structure, they could significantly improve the barrier properties, which can be attributed to the longer pathway for water vapor penetrants based on the tortuous path model [18–21].

We also measured the optical transmittance of all three samples. As shown in Fig. 4, both EIS and EZIS samples showed lower transmittance than the IS sample at a wavelength of 550 nm. However, the EZIS sample was reasonably transparent and had a greater than 85% transmittance. Therefore, the decrease in transmittance was not considered to be significant due to the remarkable enhancement of barrier properties.

We coated the epoxy-ZrP nanocomposites on the various types of inorganic layers, which had WVTR values between 10^{-1} g/m^2/day and 10^{-4} g/m^2/day. The inorganic layers were categorized as sputter A, B, C, D and ALD. Of these samples, sputter D had the same structure as IS

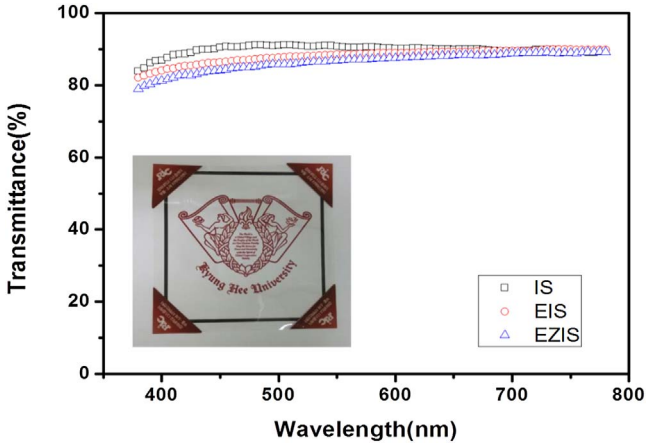

Fig. 4. Optical transmittance of each layered structure; IS, EIS and EZIS. The inset shows a photograph of the EZIS sample.

Table 1
Properties of various inorganic layers with epoxy-ZrP nanocomposite coating.

Inorganic layer	–	With epoxy-ZrP nanocomposite coating		
	WVTR (g/m^2/day)	WVTR (g/m^2/day)	ΔTrans. (%) (@ 550 nm)	ΔHaze (%)
Sputter A[a]	$4.9*10^{-1}$	$3.9*10^{-2}$	1.59	0.06
Sputter B[a]	$1.4*10^{-1}$	$1.8*10^{-2}$	-3.79	0.27
Sputter C[b]	$1.1*10^{-2}$	$3.1*10^{-3}$	-0.59	0.26
Sputter D[b]	$4.3*10^{-3}$	$8.3*10^{-4}$	-3.98	0.79
ALD[b]	$9.4*10^{-4}$	$3.7*10^{-4}$	1.68	-0.01

(*WVTR measurement – a: PERMATRAN-W 3/33, b: Ca-test).

sample mentioned above. Detailed WVTR results and optical properties are summarized in Table 1. All of the inorganic layers with epoxy-ZrP nanocomposite coating layers exhibited significantly improved barrier properties compared to those without nanocomposite coatings. Although optical transmittance decreased by about 4% after epoxy-ZrP nanocomposite coating in some cases, this is quite dependent on the optical properties of the substrate. We calculated the WVTR improvement ratio (WI) of inorganic layers after epoxy-ZrP nanocomposite coating, as defined by Eq. (1).

$$\text{WI } (\%) = (W_{IS} - W_{EZIS})/W_{IS} \times 100 \quad (1)$$

where W_{IS} is the WVTR of the bare inorganic layer and W_{EZIS} is the WVTR of theinorganic layer with an epoxy-ZrP nanocomposite coating. As shown in Fig. 5, the WI had a tendency to decrease with increasing barrier performance of the inorganic layer. This implies that the effect of the epoxy-ZrP nanocomposite coating can be offset at higher level of barrier performance [16].

Barrier films prepared in this work were applied to encapsulation of real OLED devices for validating their barrier properties. OLED devices were loaded in IVL electroluminescence characterization system, and initial luminance (L_0) was set as 2000 cd/m^2 under continuous constant current at room temperature. We have tested 4 OLED device samples; no encapsulation, IS, EZIS, and glass. Luminance decay was continuously detected for each sample, and the normalized luminescence (L/L_0) against time was plotted in Fig. 6. We defined the lifetime of OLED devices as the time required for luminance of the OLED to decline by 50% of its initial value; $L/L_0 = 0.5$. OLEDs without any encapsulation had the lifetime only about 0.6 h. However, the lifetimes of the OLED encapsulated with an IS and EZIS structure increased to 1.75 h and 9.5 h, respectively.

Even though we have not prepared OLED devices for all the samples in Fig. 5, we have confirmed the trend that barrier property of the film sample was directly related with the lifetime of OLED device. We have also tested oxygen barrier properties of some samples, and they were in

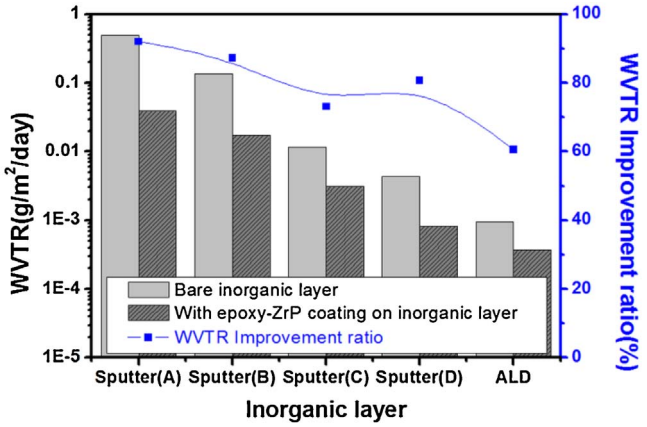

Fig. 5. A comparison of WVTR and WVTR improvement ratio with varying barrier performance level of inorganic layers.

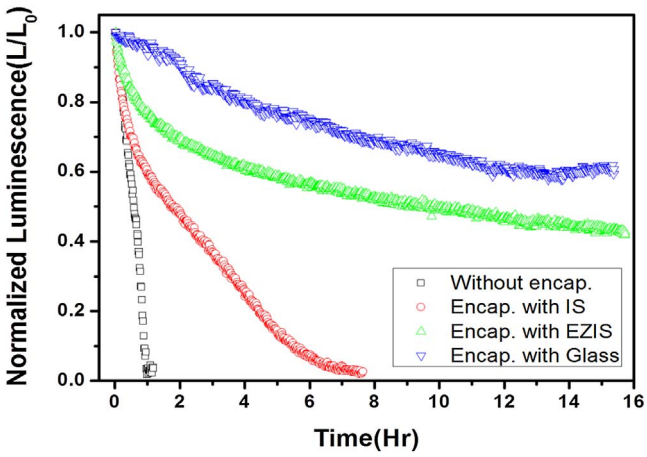

Fig. 6. Normalized luminance-time characteristics of OLEDs with various encapsulations (Starting luminance: 2000 cd/m^2).

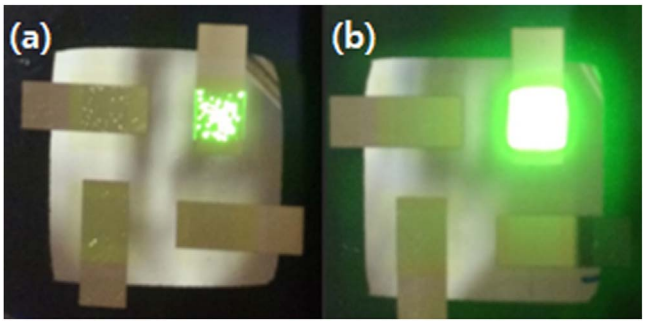

Fig. 7. Photographs of OLEDs encapsulated with (a) IS (inorganic layer/substrate) and (b) EZIS (Epoxy-ZrP nanocomposite coating/inorganic layer/substrate) samples taken after 100 h.

the similar trends to those of water vapor. OLED devices were prepared in vacuum evaporator and encapsulated in glove box, we could avoid any influence from other sources.

In addition, as shown in Fig. 7, the photographs of OLEDs taken after 100 h under ambient conditions showed that the OLED encapsulated with an EZIS structure exhibited good electroluminescent (EL) characteristics without any degradation or dark spots, while degradation and dark spots were evident in the OLED encapsulated with an IS structure.

When compared with the aforementioned Ca test results, the OLED lifetime results showed an analogous trend with respect to barrier properties. We confirmed that water permeability can be effectively reduced by an epoxy-ZrP nanocomposite coating and verified that OLED lifetime can be significantly increased by using a barrier film composed of inorganic and epoxy-ZrP nanocomposite layers.

4. Conclusions

The incorporation of an epoxy-ZrP nanocomposite coating layer on an inorganic layer deposited by sputtering or ALD significantly decreased the WVTR compared to bare inorganic layers without a nanocomposite coating, with minimal effects on the optical properties. The enhancement of the barrier properties was confirmed by the WVTR improvement ratio for various inorganic layers, which had WVTR values in the range of 10^{-1} g/m^2/day to 10^{-4} g/m^2/day, although the effect of the nanocomposite coating tended to decrease with increasing barrier performance level. The lifetime of OLEDs encapsulated with inorganic layer with the epoxy-ZrP nanocomposite coating also increased by an amount on the order of the improvement in WVTR demonstrated by the Ca test results. In conclusion, we believe that our epoxy-ZrP nanocomposite coating method is a useful and practical

method to provide high barrier performance and flexibility to various inorganic barrier materials for application in flexible organic electronic devices.

Acknowledgements

This research was supported by a grant from the Fundamental R & D Program for Technology of World Premier Materials (WPM) and by the RIC-CAMID of Kyung Hee University.

References

[1] A.R. Cho, E.H. Kim, S.Y. Park, L.S. Park, Flexible OLED encapsulated with gas barrier film and adhesive gasket, Synth. Met. 193 (2014) 77–80.
[2] C.Y. Wu, R.M. Liao, L.W. Lai, M.S. Jeng, D.S. Liu, Organosilicon/silicon oxide gas barrier structure encapsulated flexible plastic substrate by using plasma-enhanced chemical vapor deposition, Surf. Coat. Technol. 206 (2012) 4685–4691.
[3] T. Hirvikorpi, R. Laine, M. Vähä-Nissi, V. Kilpi, E. Salo, W.M. Li, S. Lindfors, J. Vartiainen, E. Kenttä, J. Nikkola, A. Harlin, J. Kostamo, Barrier properties of plastic films coated with an Al_2O_3 layer by roll-to-roll atomic layer deposition, Thin Solid Films 550 (2014) 164–169.
[4] J.G. Lee, H.G. Kim, S.S. Kim, Defect-sealing of Al_2O_3/ZrO_2 Multilayer for barrier coating by plasma-enhanced atomic layer deposition process, Thin Solid Films 577 (2015) 143–148.
[5] B.L. Danforth, E.R. Dickey, UV-curable top coat protection against mechanical abrasion for atomic layer deposition (ALD) thin film barrier coatings, Surf. Coat. Technol. 241 (2014) 142–147.
[6] N. Kim, S. Graham, Development of highly flexible and ultra-low permeation rate thin-film barrier structure for organic electronics, Thin Solid Films 547 (2013) 57–62.
[7] D.A. Spee, J.K. Rath, R.E.I. Schropp, Using hot wire and initiated chemical vapor deposition for gas barrierthin film encapsulation, Thin Solid Films 575 (2015) 67–71.
[8] D. Feldman, Review polymer nanocomposite barriers, J. Macromol. Sci. Part A: Pure Appl. Chem. 50 (2013) 441–448.
[9] D.A. Kunz, J. Schmid, P. Feicht, J. Erath, A. Fery, J. Breu, Clay-based nanocomposite coating for flexible optoelectronics applying commercial polymers, ACS Nano 7 (2013) 4275–4280.
[10] B.M. Yoo, H.J. Shin, H.W. Yoon, H.B. Park, Review Graphene and graphene oxide and their uses in barrier polymers, J. Appl. Polym. Sci. 131 (2014) 39628.
[11] L. Sun, W.J. Boo, H.J. Sue, A. Clearfield, Preparation of α-zirconium phosphate nanoplatelets with wide variations in aspect ratios, New J. Chem. 31 (2007) 39–43.
[12] M.D. Kempe, M.O. Reese, A.A. Dameron, Evaluation of the sensitivity limits of water vapor transmission rate measurements using electrical calcium test, Rev. Sci. Instrum. 84 (2013) 025109.
[13] R. Paetzold, A. Winnacker, D. Henseler, V. Cesari, K. Heuser, Permeation rate measurements by electrical analysis of calcium corrosion, Rev. Sci. Instrum. 74 (2003) 5147–5150.
[14] E. Kim, Y. Han, W. Kim, K.C. Choi, H.G. Im, B.S. Bae, Thin film encapsulation for organic light emitting diodes using a multi-barrier composed of MgO prepared by atomic layer deposition and hybrid materials, Org. Electron. 14 (2013) 1737–1743.
[15] D. Yu, W. Xiao, D.Y. Hui, Y.Y. Qiang, C. Ping, Y. Dan, S.F. Bo, X.K. Wen, H. Nan, H.J. Wen, High-performance barrier using a dual-layer inorganic/organic hybrid thin-film encapsulation for organic light-emitting diodes, Org. Electron. 15 (2014) 1936–1941.
[16] Y.J. Park, H.G. Kim, E.H. Kim, S.S. Kim, Enhancement of barrier property of plastic substrate by intra-gallery polymerization for nanocomposites, Macromol. Res. 22 (2014) 67–73.
[17] M.A. Osman, V. Mittal, M. Morbidelli, U.W. Suter, Epoxy-layered silicate nanocomposites and their gas permeation properties, Macromolecules 37 (2004) 7250–7257.
[18] R.K. Bharadwaj, Modeling the barrier properties of polymer-layered silicate nanocomposites, Macromolecules 34 (2001) 9189–9192.
[19] A.A. Azzez, K.Y. Rhee, S.J. Park, D. Hui, Epoxy clay nanocomposites – processing, properties and applications: a review, Compos. Part B 45 (2013) 308–320.
[20] L. Sun, W.J. Boo, A. Clearfield, H.J. Sue, H.Q. Pham, Barrier properties of model epoxy nanocomposites, J. Membr. Sci. 318 (2008) 129–136.
[21] M. Wong, R. Ishige, K.L. White, P. Li, D. Kim, R. Krishnamoorti, R. Gunther, T. Hiquchi, H. Jinnai, A. Takahara, R. Nishimura, H.J. Sue, Large-scale self-assembled zirconium phosphate smectic layers via a simple spray-coating process, Nat. Commun. 5 (2014) 3589.